Journal of Cellular Biochemistry 97:1379–1392 (2006)

$PGF_{2\alpha}$ Increases FGF-2 and FGFR2 Trafficking in Py1a Rat Osteoblasts Via Clathrin Independent and Importin β Dependent Pathway

Luigi Marchetti,[1]* Maria G. Sabbieti,[1] Dimitrios Agas,[1] Maura Menghi,[2] Giovanni Materazzi,[1] Giovanna Menghi,[1] and Marja M. Hurley[3]

[1]Department of Comparative Morphology and Biochemistry, University of Camerino, Camerino (MC)/Italy
[2]Dia Tech Lab, Jesi (AN)/Italy
[3]Division of Endocrinology and Metabolism, University of Connecticut Health Center, Farmington, Connecticut

Abstract Previous studies showed that prostaglandin $F_{2\alpha}$ ($PGF_{2\alpha}$) stimulated fibroblast growth factor-2 (FGF-2) and fibroblast growth factor receptor 2 (FGFR2) cytosolic and nuclear accumulation, however, the endocytic pathway has not been elucidated. This study demonstrates that although $PGF_{2\alpha}$ increased the formation of clathrin-coated structures in Py1a rat osteoblasts, they were not involved in FGF-2 and FGFR2 trafficking. $PGF_{2\alpha}$ increased binding of FGF-2 and FGFR2 and co-localization of reactive sites in addition to nuclear translocation at the nuclear pore complex level. FGF-2 and FGFR2 were in close spatial correlation with importin β, further supporting nuclear import of the FGF-2/FGFR2 complex. Immunogold and immunofluorescence techniques as well as Western blotting demonstrated increased importin β protein labeling in response to $PGF_{2\alpha}$. Similar to $PGF_{2\alpha}$, phorbol 12-myristate 13-acetate (PMA) also increased importin β protein. These data strongly suggest that prostaglandins may regulate osteoblast metabolism via FGF-2/FGFR2/importin β nuclear trafficking. J. Cell. Biochem. 97: 1379–1392, 2006.

Key words: $PGF_{2\alpha}$; FGF-2; FGFR2; rat osteoblasts; clathrin; importin β; TEM; CLSM; Western blotting

Prostaglandins (PGs) have important effects on bone metabolism participating in bone formation and bone resorption [Raisz and Martin, 1983; Pilbeam et al., 2002]. Prostaglandin E_2 stimulates bone formation in vivo at low concentration [Norrdin et al., 1990], while high concentration of PGE_2 inhibits collagen synthesis in organ cultures and in clonal osteoblastic cell lines [Raisz and Fall, 1990; Raisz et al., 1993]. Basic fibroblast growth factor (bFGF or FGF-2) is a member of a heparin binding growth factor family. Binding to heparin also stabilizes FGF-2 and potentiates its bioactivity [Saksela et al., 1988]. FGF-2 signals via high affinity tyrosine kinase FGF receptors (FGFRs) that are involved in many biological processes during embryo development and homeostasis of body tissues. Disruption of normal FGF receptor functions lead to pathological conditions in humans [Groth and Lardelli, 2002].

Together with FGF-2 and FGFRs [Hurley et al., 2002], PGs are major modulators of bone cell function [Pilbeam et al., 2002]. We previously reported that prostaglandin $F_{2\alpha}$ ($PGF_{2\alpha}$) and Fluprostenol (Flup), regulate the expression of FGF-2 in immortalized rat osteoblastic Py1a cells by a protein kinase C (PKC)-mediated mechanism and are able to induce nuclear translocation of FGF-2 [Sabbieti et al., 2001]. In other study, we demonstrated that PGs increased FGF-2 mRNA and protein in bone cells; in particular, immunogold labeling on ultrathin sections from calvariae showed that stimulation with PGs caused a transition of

Grant sponsor: University of Camerino and Fondazione Carima, Italy; Grant sponsor: NIH; Grant number: AG21189.

*Correspondence to: Prof. Luigi Marchetti, Department of Comparative Morphology and Biochemistry, University of Camerino, via Gentile III da Varano, 10, I-62032 Camerino (MC)/Italy. E-mail: luigi.marchetti@unicam.it

Received 14 July 2005; Accepted 24 October 2005
DOI 10.1002/jcb.20746

FGF-2 from bone matrix to cells and an increased cytoplasmic labeling in periosteal cells and in osteoblasts [Sabbieti et al., 1999]. Moreover, confocal (CLSM) and electron microscopy (TEM) showed that under $PGF_{2\alpha}$ stimulation, FGF-2 and FGFR2 proteins accumulated near the nuclear envelope of Py1a cells by a protein kinase C-mediated pathway involving MAPK/ERK2 [Sabbieti et al., 2005].

In the present study, we investigated the endocytic/trafficking pattern and immunolocalization of FGF-2 and its receptor 2 in Py1a rat osteoblasts in response to $PGF_{2\alpha}$ stimulation. Specifically, the relation between these proteins and clathrin-coated structures was examined. Indeed, endocytosis plays a critical role in cellular functions, and in particular, receptor-mediated endocytosis allows the specific removal of cell surface receptors and their cargo from the plasma membrane [Pearse and Robinson, 1990]. In particular, clathrin-dependent endocytosis is the best-defined process so far and it is responsible for the rapid uptake of molecules including several growth factors [Rodal et al., 1999]. This process starts with the formation of clathrin-coated pits that initiates the budding of clathrin-coated vesicles from membrane [Schmid, 1997]. The nuclear translocation of FGFR2 and FGF-2 was also investigated at TEM level. Nuclear import and export are reported to involve nuclear pore complexes (NPC) and can occur along multiple distinct pathways [Nakielny and Dreyfuss, 1999]. Importin β is a soluble protein trafficking between the cytoplasm and the nucleus and it is a critical component of multiple nuclear import pathways mediated by transport receptors [Görlich and Kutay, 1999; Conti and Izaurralde, 2001].

We previously hypothesized that $PGF_{2\alpha}$ increased FGF-2 mRNA and, after its translation, FGF-2 protein binds FGFR2 and is translocated into the nucleus [Sabbieti et al., 2005]. In the present research, we suggest that the nuclear translocation of FGFR2 and FGF-2 is mediated by importin β.

MATERIALS AND METHODS

Cell Cultures for TEM

Py1a cells were cultured following the protocol described by Sabbieti et al. [2005]. Then, cells were stimulated with $PGF_{2\alpha}$ (10^{-5} M) (Sigma-Aldrich srl, Milano, Italy) for 6 h and 24 h. Control cultures were pulsed with appropriate vehicle.

Ultrastructural analysis. After two rinsing in F-12 medium and one quick washing in 0.1 M cacodylate buffer, pH 7.4, cells were fixed on plates with 4% paraformaldehyde and 2.5% glutaraldehyde in 0.1 M cacodylate buffer containing 2.5 mM $CaCl_2$ for 3 h at 4°C. Then, cells were rinsed several times in 0.1 M cacodylate buffer for 30 min at 4°C and post-fixed in 1% OsO_4 in 0.1 M cacodylate buffer for 1 h at 4°C. Cacodylate buffer was then replaced with 0.1 M phosphate-buffered saline solution (PBS), pH 7.3, containing 0.1% BSA and 7% sucrose and cells were rinsed four times (15 min each) at 4°C. Cells were subsequently scraped and collected in Falcon tubes. The centrifuged cells (1,300 rpm for 4 min) were placed on 2.6% agarose and, after centrifugation, cells pre-embedded in agarose were dehydrated in ascending concentrations of methanol, passed through propylene oxide, and embedded in Embed 812 (Electron Microscopy Sciences, Fort Washington, PA) for 48 h at 60°C.

Ultrathin sections (about 50 nm thick) were cut by means of a LKB Ultrotome V and collected on Formvar-coated 200 mesh nickel grids. Sections were finally counterstained with uranyl acetate (4 min) and lead citrate (3 min) at room temperature.

Immunoelectron microscopy. After two rinsing in F-12 medium and one quick washing in 0.1 M cacodylate buffer, pH 7.4, cells were fixed, collected, and embedded in Unicryl resin (BBInternational Ltd., Cardiff, UK) as described in Sabbieti et al. [2005].

Single and double-sided binding for FGF-2, FGFR1, FGFR2. Single immunogold binding for FGF-2 and FGFR2 was performed following the protocol described in Sabbieti et al. [2005]. In addition, a polyclonal goat anti-C-term-FGFR1 antibody (Flg C-15, Santa Cruz Biotechnology, Inc., California) was tested at a dilution ranging from 1:5 up to 1:160 in 0.05 M Tris buffered saline solution (TBS), pH 7.6, containing 1% BSA overnight at 4°C in a humid chamber.

In the double-sided binding experiments, sections were FGFR2-labeled as above on one face (face A) and then gold particles were enhanced for 6 min at room temperature by means of a silver enhancing kit (BBInternational Ltd.). After rinsing in distilled water, the reacted grid face (face A) was covered by a

Formvar film (0.15% in 1,2-Dichloroethane) to avoid reagent contamination. Then, grid was turned out and the opposite face (face B) was incubated with polyclonal rabbit anti-FGF-2 antibody as above.

In order to establish the presence of co-localized or exclusive sites, and to control the accuracy of the procedure, the double-sided method was also performed by reversing the sequence of labeling on the two faces.

Single and double-sided binding for clathrin, FGF-2, FGFR2. Floating ultrathin sections were rehydrated with 0.05 M TBS, pH 7.6, and pre-incubated with 5% normal goat serum in 0.05 M TBS, pH 7.6, for 30 min at room temperature. Grids were then incubated with monoclonal anti-clathrin heavy chain (Sigma-Aldrich srl) at a concentration of 8 μg/ml in 0.05 M TBS, pH 7.6, overnight at 4°C in a humid chamber, and the signal was developed with goat anti-mouse IgG 10 nm gold conjugated (Sigma-Aldrich srl) diluted 1:10 in 0.05 M TBS, pH 7.6, for 2 h at 4°C in a humid chamber. Sections were then washed several times in 0.05 M TBS, pH 7.6, and in distilled water.

In the double-sided binding experiments, sections were labeled for FGF-2 or FGFR2 as above described and then gold particles were enhanced for 6 min at room temperature by means of a silver enhancing kit (BBInternational Ltd.). After rinsing in distilled water, the reacted grid face (face A) was covered by a Formvar film (0.15% in 1,2-Dichloroethane). Then, grid was turned out and the opposite face (face B) was incubated with monoclonal anti-clathrin heavy chain (Sigma-Aldrich srl) as above.

Double-sided binding for importin β, FGF-2, and FGFR2. Ultrathin sections were labeled for FGF-2 or FGFR2 as above. After rinsing in distilled water, the reacted grid face (face A) was covered by a Formvar film (0.15% in 1,2-Dichloroethane). After binding of face A, the grid was turned out and face B was incubated with Mab to Nuclear Transport Factor p97 (importin β) (Vinci-Biochem, Vinci, Italy) diluted 1:300 in 0.05 M TBS, pH 7.6, containing 1% BSA overnight at 4°C in a humid chamber. The signal was then developed with a goat anti-mouse IgG (H + L) 40 nm gold conjugated (BBInternational Ltd.) diluted 1:15 in 0.05 M TBS, pH 7.6, containing 0.05% Tween 20 for 90 min at room temperature in a humid chamber.

In order to establish the presence of co-localized or exclusive sites and verify the accuracy of the procedure, double-sided binding method was also performed by reversing the sequence of labeling on the two faces.

All sections were finally counterstained with uranyl acetate (5 min) and lead citrate (2 min) at room temperature.

All specimens were analyzed by means of a Philips EM 201C electron microscope at an accelerating voltage of 60 kV.

Image Analysis for FGF-2, FGFR2, and Importin β

Image analysis was performed on Scion Image Beta 4.03 for Windows XP.

The electronic microscopic images of Py1a cells treated for 24 h with $PGF_{2\alpha}$ or pre-treated with PMA before administration of $PGF_{2\alpha}$ for 24 h were scanned by the computer. The labeling density was then estimated on nuclei of 16 samples in each experimental group. In particular, we measured the FGF-2/importin β and FGFR2/importin β co-localized gold signals. Values were referred as mean ± standard deviation (SD) and statistically analyzed with *t*-test operating on PC computer.

Cell Cultures for CLSM

Immortalized rat Py1a osteoblasts were cultured as described in a previous research [Sabbieti et al., 2000] before treatment with $PGF_{2\alpha}$ (10^{-5} M) for 6 and 24 h. Control cultures were treated with appropriate vehicles.

Double binding for importin β, FGF-2, and FGR2. After stimulation, cells were fixed and permeabilized as described in Sabbieti et al. [2000]. Then, cells were incubated with the polyclonal rabbit anti-FGF-2 antibody diluted 1:100 in PBS or with polyclonal rabbit anti-FGFR2 antibody (Santa Cruz Biotechnology, Inc., CA) diluted 1:50 in PBS and the Mab to Nuclear Transport Factor p97 diluted 1:400 in PBS, for 2 h at room temperature. After rinsing, cells were incubated with goat anti-rabbit IgG conjugated with fluorescein isothiocyanate (FITC) diluted 1:60 in PBS and with Alexa Fluor 594 goat anti-mouse (Molecular Probes, Inc., Eugene, OR) diluted 1:40 for 90 min at room temperature. After washing, coverslips were mounted on slides with PBS/glycerol (1:1). Finally, CLSM analysis was performed as previously detailed [Menghi et al., 1997]. Sections were examined and original images were stored as a PIC format file and then printed with

an Epson Stylus Photo 890 on Epson glossy photo paper.

All control experiments at TEM and CLSM level were carried out by omitting the appropriate primary antibodies, or by complexing the primary antibodies with the relative blocking peptide.

Western blot analysis for importin β. Py1a cells were plated at 5,000 cells/cm^2 in 100 mm culture dishes in F-12 culture medium with 5% nonheat inactivated fetal calf serum, penicillin, and streptomycin. Cells were grown for 5 days up to 80% of confluence. Then, cells were serum deprived 24 h before addition of $PGF_{2\alpha}$ (10^{-5} M) and phorbol 12-myristate 13-acetate (PMA) (10^{-6} M) for 24 h. Parallel cultures were pre-treated with PMA for 24 h before adding the effectors.

Proteins were extracted with Cytobuster Protein extraction reagent (Inalco SPA, Milano, Italy). Proteins determination were performed with 2D-Quant kit (Amersham Biosciences Europe GMBH, Cologno Monzese, Italy) and an equal amount of proteins was resolved by SDS–PAGE (12%) and transferred onto PVDF (Hybond-P) membrane (Amersham Biosciences Europe GMBH). The next steps were performed by ECL Advance Western Blotting Detection Kit (Amersham Biosciences Europe GMBH). Briefly, membranes were blocked with Advance Blocking agent in PBS-T (PBS containing 0.1% Tween 20) for 1 h at room temperature. Then, membranes were incubated with the Mab to Nuclear Transport Factor p97 diluted 1:2,500 for 1 h at room temperature. After washing with PBS-T the blots were incubated with horseradish peroxidase (HRP)-conjugated sheep anti-mouse IgG (Amersham Biosciences Europe GMBH) diluted 1:100,000 in blocking solution for 1 h at room temperature. After further washing with PBS-T, immunoblot was developed with luminol reagents and exposed to Hyperfilm-ECL film (Amersham Biosciences Europe GMBH) according to the manufacturer's instructions. Then filters were stripped and riprobed with a monoclonal Anti- α-tubulin, mouse ascites fluid (Sigma-Aldrich srl) to show equal amount of loading.

RESULTS

Effects of $PGF_{2\alpha}$ on Cell Ultrastructure

Vehicle-treated Py1a cells often appeared fusiform in shape and showed an elongated nucleus presenting electron-transparent chromatin dispersed in less abundant electron-dense one. Cells were characterized by numerous and elongated mitochondria and abundant rough endoplasm reticulum (RER) sometime showing dilated cisternae. Some lipid droplets were also observed. A small amount of plasma membrane area showed superficial thickness and formation of coated pit regions (Figs. 1 and 2). Py1a cells stimulated for 24 h with $PGF_{2\alpha}$ showed an increase of coated pit- and coated vesicle-structures. It was possible to distinguish shallow pits, which are flattened or only slightly invaginated (Fig. 3a, b); invaginated pits, that is, when the pits are clearly invaginated but the necks connecting them with the exterior are still open wide (slightly wider or narrower than the diameter of the pit itself) (Fig. 3c); and pits that are almost or completely

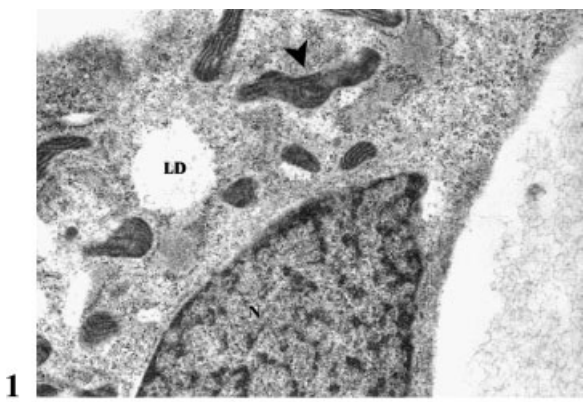

1

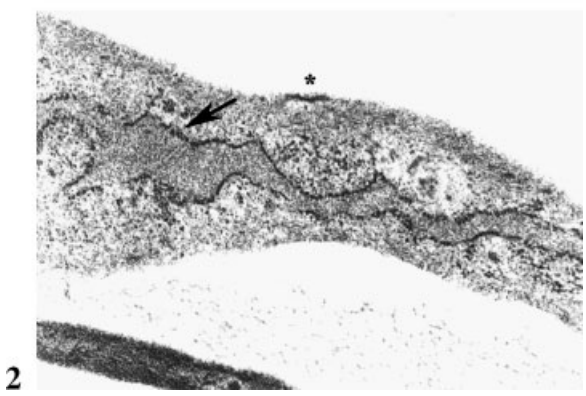

2

Fig. 1. Ultrastructure of Py1a rat osteoblasts. The cell is characterized by fusiform shape, a smooth nuclear outline, and a cytoplasm rich in elongated mitochondria (arrowhead) and in rough endoplasmic reticulum (RER). Nucleus (N). Lipid droplet (LD). 15,100×.

Fig. 2. Ultrastructure of Py1a rat osteoblasts. Sometimes dilated regions of RER were observed (arrow). Coated pit structure (asterisk). 30,600×.

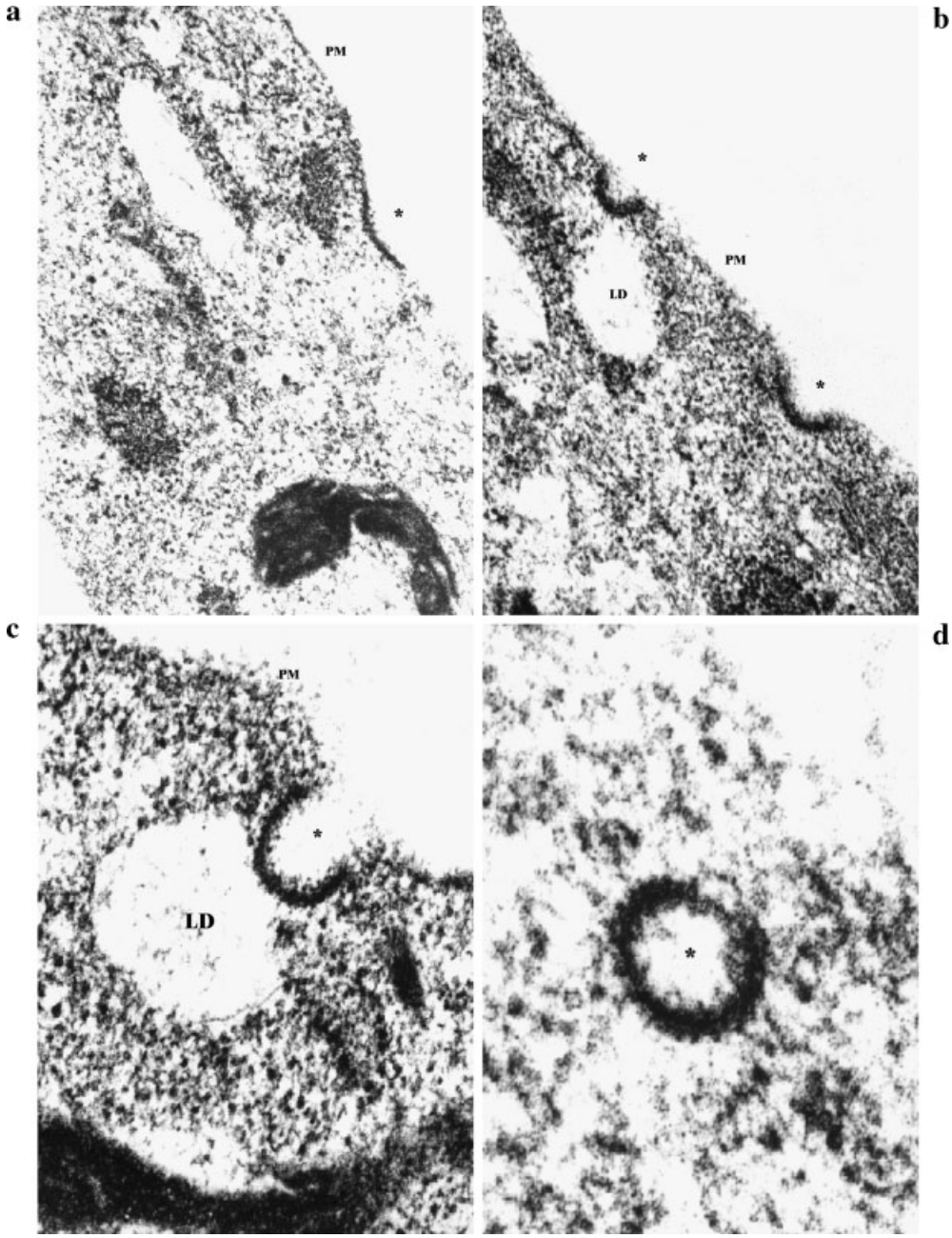

Fig. 3. **a, b, c, d**: Ultrastructure of thin cross sections of Py1a rat osteoblasts stimulated for 24 h with $PGF_{2\alpha}$. Portion of plasma membrane and cytoplasm showing representative examples of coated pit structures at various degree of invagination (a–c). An apparently free coated vesicular profile is shown in d. Plasma membrane (PM). Coated pits and/or coated vesicles structures (asterisks). Lipid droplet (LD). a, b: 59,400×; c: 92,400×; d: 98,500×.

pinched off (Fig. 3d). Stimulated cells also showed increased RER dilated cisternae and prominent nucleolus.

Effects of $PGF_{2\alpha}$ on FGF-2/FGFR2 Localization and Clathrin-Coated Pits and Vesicles

To determine the nature of pits and vesicles observed at ultrastructural level, we carried out immunogold labeling experiments on ultrathin sections. By means of a monoclonal anti-clathrin antibody, punctate labeling was seen at the periphery of osteoblasts, particularly along pits (Fig. 4a) or vesicles (Fig. 4b).

In unstimulated cells and after 6 h of $PGF_{2\alpha}$ treatment, labeling of FGF-2 and FGFR2 was primarily observed in the cytoplasm, but they

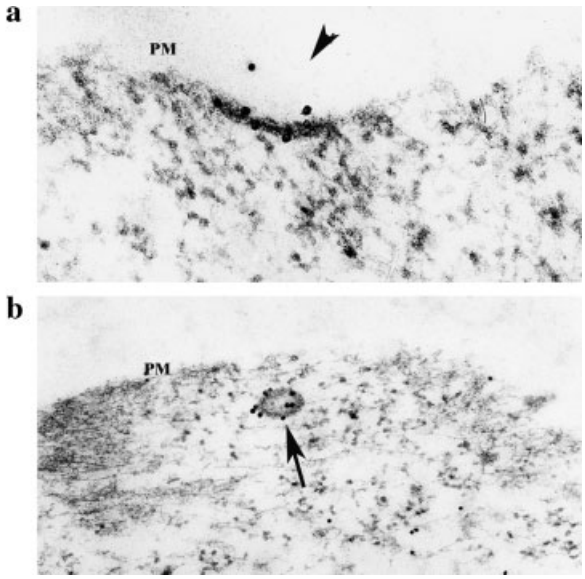

Fig. 4. a, b: Immunogold staining of clathrin in Py1a rat osteoblasts stimulated for 24 h with $PGF_{2\alpha}$. The immunoreactivity with monoclonal anti-clathrin heavy chain was detected with goat anti-mouse IgG 10 nm gold conjugated. Clathrin was visualized in pits (arrowhead) (a) and vesicles (arrows) (b). Plasma membrane (PM). (a) 87,100×; (b) 42,300×.

were not co-localized (Fig. 5a,b). After 24 h of $PGF_{2\alpha}$ stimulation, cells showed striking perinuclear and nuclear labeling of both proteins and double-sided binding confirmed a co-localization of FGF-2 and FGFR2 (Fig. 6a,c). These results were also confirmed by reversing the sequence of labeling on the two faces of the grid (Fig. 6b). Importantly, although treatment with $PGF_{2\alpha}$ increased clathrin-coated pits and vesicles, they seemed to be not involved in the transport of FGF-2 (Fig. 7a) or FGFR2 (Fig. 7b). In cells stimulated for 24 h with $PGF_{2\alpha}$, we also noted the localization of FGF-2 (Fig. 8) and its receptor 2 (Fig. 9) at the level of the nuclear pore complex and inside the nucleus.

Effects of $PGF_{2\alpha}$ on FGF-2/FGFR2/ Importin β Localization

We next examined whether importin β levels were modulated by $PGF_{2\alpha}$ and were involved in FGF-2 and FGFR2 nuclear translocation. Double-sided binding performed on Py1a cells stimulated for 24 h with $PGF_{2\alpha}$ showed a close relation between importin β and FGF-2 (Fig. 10) or between importin β and FGFR2 (Fig. 11) at nuclear envelope and inside the nucleus. CLSM further supported TEM data and indicated that

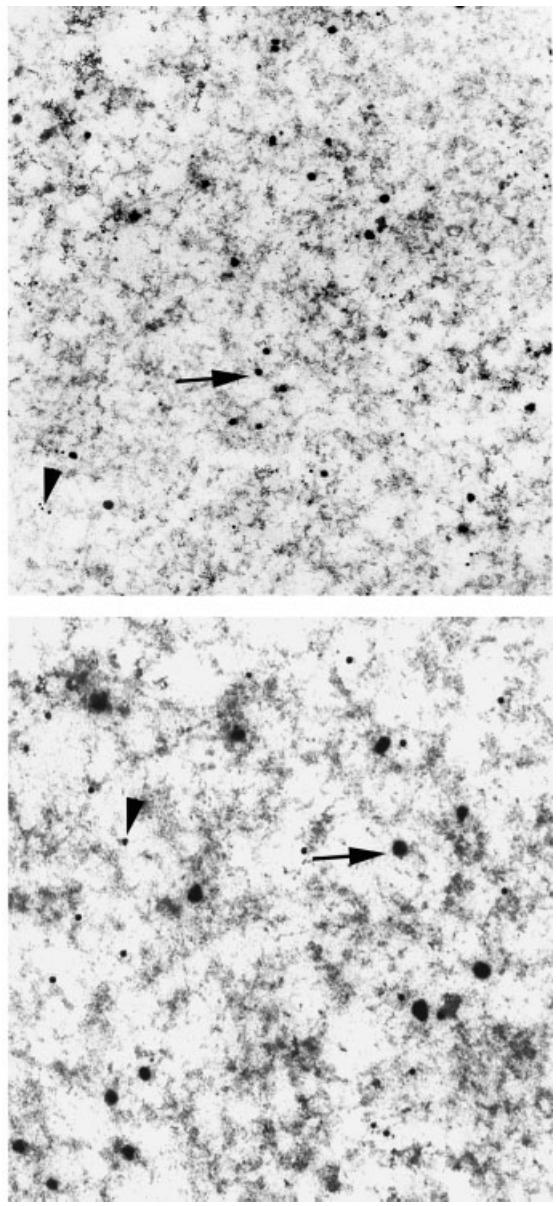

Fig. 5. a, b: Double-sided binding of FGF-2 and FGFR2 in unstimulated Py1a osteoblasts. The immunoreactivity with rabbit anti-FGF-2 or with goat anti-C-term-FGFR2 was detected with silver enhanced 10 nm colloidal gold particles conjugated to goat anti-rabbit IgG and with rabbit anti-goat IgG 10 nm gold conjugated, respectively. a: The cytoplasmic sparse labeling of both FGF-2, small particles (arrowhead), and FGFR2, large particles (arrow), did not present co-localization. b: A higher magnification better depict the absence of co-localized sites. a: 31,400×; (b) 55,800×.

the accumulation of FGF-2 and importin β begins at 6 h of $PGF_{2\alpha}$ stimulation. At around 24 h of treatment, the nuclear co-localization of both proteins (Fig. 12a–c), was detailed in the magnification of a single cell (Fig. 12a–c insets),

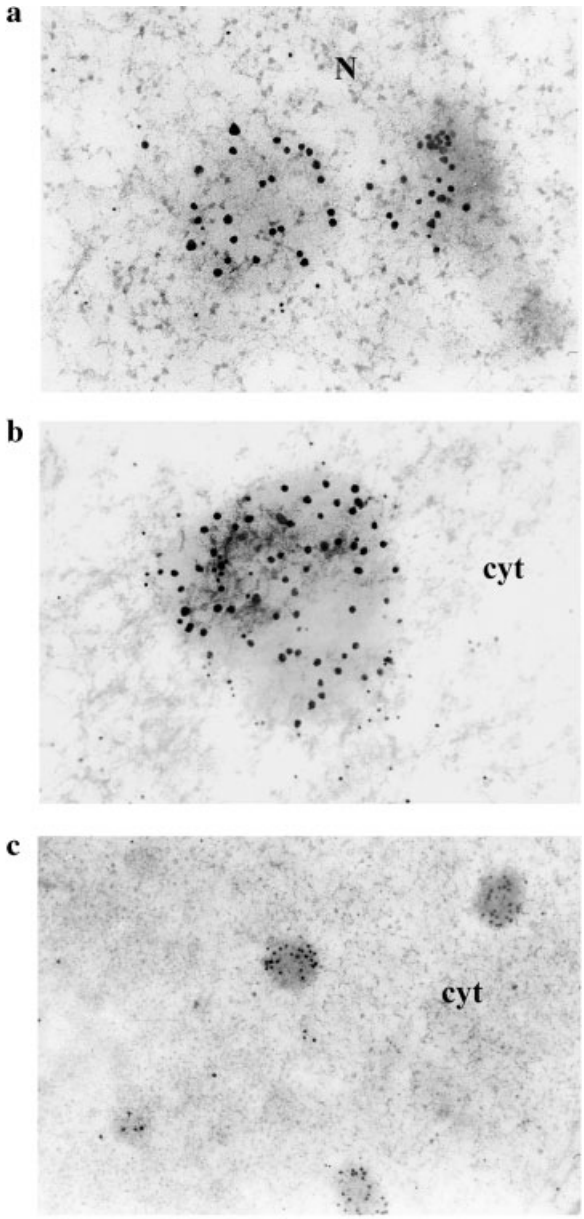

Fig. 6. a, b, c: Double-sided binding of FGF-2 and FGFR2 in Py1a osteoblasts stimulated for 24 h with $PGF_{2\alpha}$. a: Co-localization of FGF-2 (small particles) and FGFR2 (large particles). b: The reverse reaction showed similar binding patterns. c: Co-localization of FGF-2 (small particles) and FGFR2 (large particles). A smaller magnification better clarify that the patchy distribution and co-localization are the predominant patterns observed in stimulated cells. Nucleus (N); cytoplasm (cyt), (a), (b) 33,200×; (c) 17,200×.

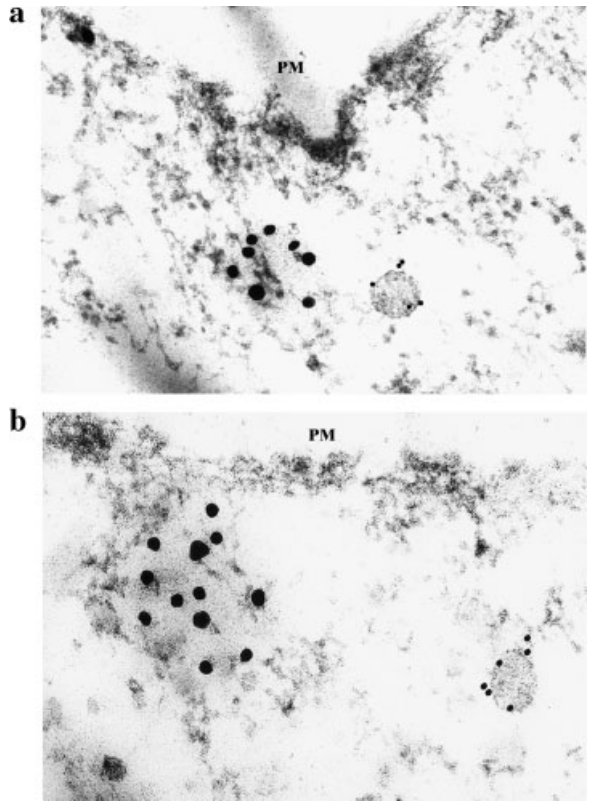

Fig. 7. a, b: Double-sided binding of FGF-2/FGFR2 and clathrin in Py1a osteoblasts stimulated for 24 h with $PGF_{2\alpha}$. The immunoreactivity with rabbit anti-FGF-2 or with monoclonal anti-clathrin heavy chain was detected with silver enhanced 10 nm colloidal gold particles conjugated to goat anti-rabbit IgG and to goat anti-mouse IgG 10 nm gold conjugated (a). The immunoreactivity with goat anti-C-term-FGFR2 or with monoclonal anti-clathrin heavy chain was detected with silver enhanced 10 nm colloidal gold particles conjugated to rabbit anti-goat IgG and to goat anti-mouse IgG 10 nm gold conjugated. Distinct localization of FGF-2 (large particles) and clathrin (small particles) (a) as well as of FGFR2 (large particles) and clathrin (small particles) (b) was observed. Plasma membrane (PM). a: 51,300×; (b) 55,600×.

where the optical sections indicated that both proteins co-localized in the nucleus. Similar results were also obtained for FGFR2. Differently from untreated Py1a osteoblasts (Fig. 13a–c), after 24 h of treatment with $PGF_{2\alpha}$, clear evidences of co-localization of FGFR2 and importin β at nuclear level were observed (Fig. 14a–c). Since we previously observed that PMA-regulated FGF-2 and FGFR2 nuclear accumulation in Py1a cells [Sabbieti et al., 1999, 2005], we also examined the effect of PMA on importin β pathway. FGF-2 and FGFR2 nuclear accumulation was prevented by PMA pre-treatment before administration of $PGF_{2\alpha}$ for 24 h [Sabbieti et al., 2005]. At TEM level, the double labeling FGF-2/importin β (Fig. 15) or FGFR2/importin β (Fig. 16) showed that importin β seemed to not co-localize with the two proteins in PMA pre-treated cells. Statistical analysis of nuclear binding (Fig. 17)

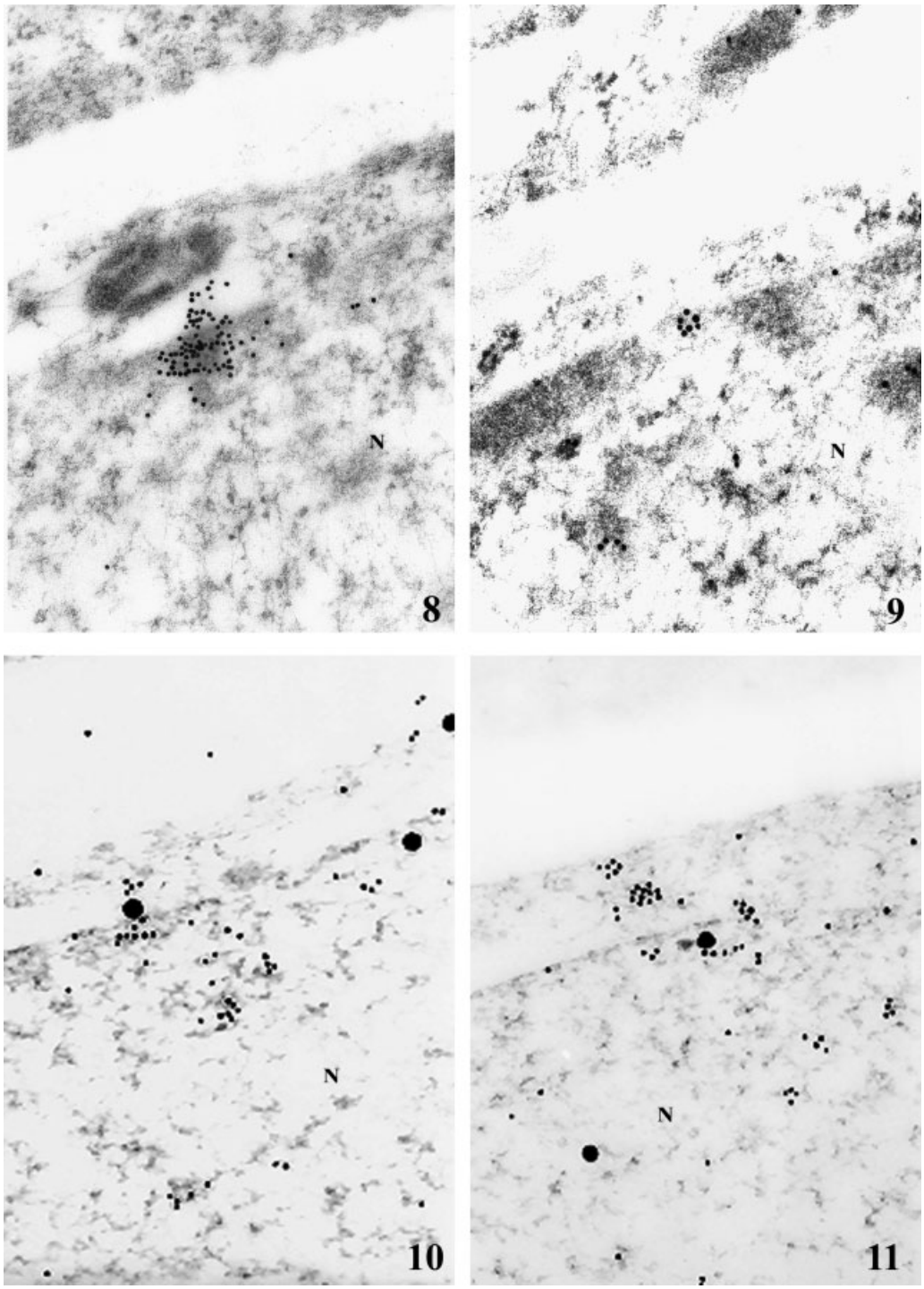

Fig. 8. Immunogold labeling of FGF-2 in Py1a osteoblasts stimulated for 24 h with $PGF_{2\alpha}$. The immunoreactivity with rabbit anti-FGF-2 was detected with goat anti-rabbit IgG 10 nm gold conjugated. To note the presence of gold signals at nuclear pore complex. Nucleus (N). 57,000×.

Fig. 9. Immunogold labeling of FGFR2 in Py1a osteoblasts stimulated for 24 h with $PGF_{2\alpha}$. The immunoreactivity with goat anti-C-term-FGFR2 was detected with rabbit anti-goat IgG 10 nm gold conjugated. To note the presence of gold signals also inside the nucleus (N). 59,100×.

Fig. 10. Double-sided binding of importin β and FGF-2 in Py1a osteoblasts stimulated for 24 h with $PGF_{2\alpha}$. The immunoreactivity with Mab to Nuclear Transport Factor p97 or with rabbit anti-FGF-2 was detected with goat anti-mouse IgG 40 nm gold conjugated and with goat anti-rabbit IgG 10 nm gold conjugated, respectively. Nucleus (N). 59,250×.

Fig. 11. Double-sided binding of importin β and FGFR2 in Py1a osteoblasts stimulated for 24 h with $PGF_{2\alpha}$. The immunoreactivity with Mab to Nuclear Transport Factor p97 or with goat anti-C-term-FGFR2 was detected with goat anti-mouse IgG 40 nm gold conjugated and with rabbit anti-goat IgG 10 nm gold conjugated, respectively. Nucleus (N). 58,600×.

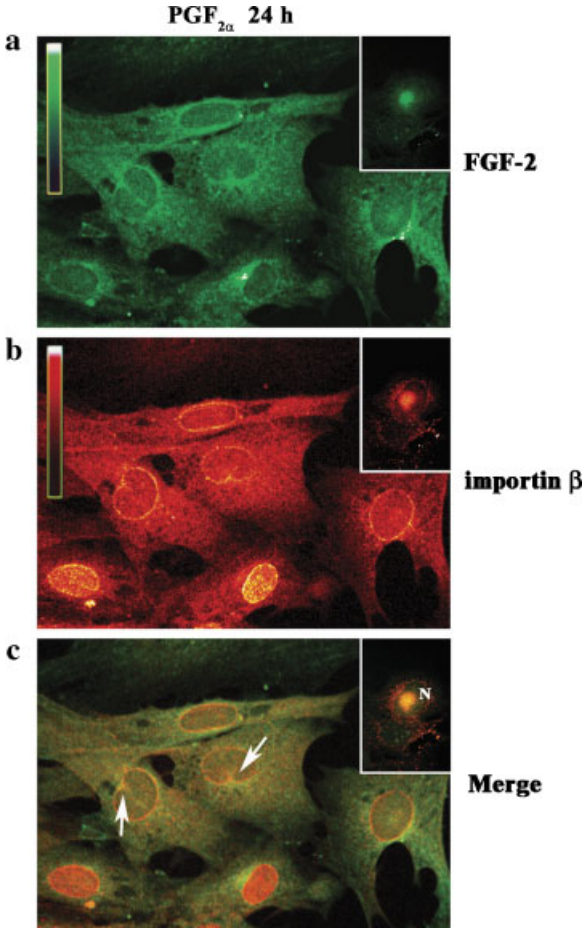

Fig. 12. a, b, c: Py1a osteoblasts treated for 24 h with $PGF_{2\alpha}$. Optical section obtained by a Bio-Rad MRC-600 Confocal Laser Scanning Microscope (CLSM). Micrographs showing cells double stained with FGF-2 (green: FITC staining) (a) and importin β (red: Alexa Fluor 594 staining) (b). Co-localization of the two signals corresponding to FGF-2 and importin β, assessed by confocal analysis of single optical sections, is shown in yellow pseudo color in the merged image (c). The intensity-coded scales, with white being the most intense, are shown on the left. Co-localized sites occurred at perinuclear region level, traversing the nuclear envelope in restricted regions (arrows) or inside the nucleus (Fig. 12a–c, insets). Nucleus (N). 450×; insets 750×. [Color figure can be viewed in the online issue, which is available at www.interscience.wiley.com.]

showed that co-localization of FGF-2/importin β and FGFR2/importin β felt down in PMA pre-treated cells. The mean labeling density of FGF-2/importin β and FGFR2/importin β was $0.5 \pm 0.5/\mu m^2$ and $0.25 \pm 0.5/\mu m^2$, respectively; $P < 0.05$.

To further investigate the role of importin β, 5′-deoxy-5′methyl-thioadenosine (MTA) (Sigma-Aldrich srl) was used. The pre-treatment with MTA (20 min at 37°C, 3 μM/ml) was carried out to prevent FGFRs activation [Chua et al., 2004]. An evident reduction of FGFR2 labeling was observed in MTA pre-treated cells (Fig. 18a), and was not modified after treatment with $PGF_{2\alpha}$ for 24 h (Fig. 19a) indicating that $PGF_{2\alpha}$ effects are depending on FGFR2 activation. Although, MTA pre-treatment only slightly affected importin β occurrence and distribution (Figs. 18b and 19b), we did not observe co-localization of both protein into the nucleus.

No gold particles or fluorescence were observed in control experiments (data not shown).

Western blot analysis was performed to provide additional information about importin β behavior in $PGF_{2\alpha}$ stimulated cells. Since we previously observed that PMA-regulated FGF-2 and FGFR2 nuclear accumulation in Py1a cells [Sabbieti et al., 1999, 2005], we also examined the effect of PMA on importin β pathway. Immunoblotting experiments demonstrated that 24 h of treatment with $PGF_{2\alpha}$ and PMA increased importin β levels. However, 24 h of pre-treatment with PMA prevented any additional increases induced by the subsequent $PGF_{2\alpha}$ or PMA treatment (Fig. 20).

DISCUSSION

Py1a rat osteoblasts exhibited the ultrastructural features of metabolically active cells. In addition, these cells contained cytoplasmic lipid droplet structures similar to those described by other authors [Yu et al., 1998, 2000; Prattes et al., 2000; Fujimoto et al., 2001; Akimoto et al., 2002]. Such lipid droplets were never found to label FGF-2 and/or its receptor 2. The cell membrane of Py1a osteoblasts showed the presence of coated pit- and coated vesicle structures that increased after 24 h of stimulation with $PGF_{2\alpha}$. Immunogold experiments demonstrated that these structures were of clathrin coated origin. However double-sided binding studies showed that in unstimulated or $PGF_{2\alpha}$-stimulated cells, there was no co-localization of FGF-2 or FGFR2 and clathrin, suggesting that the entry of both proteins occurred via clathrin-independent mechanisms. Other investigators have also reported that endocytosis could occur by clathrin-independent mechanisms [van Deurs et al., 1989; Sandvig and van Deurs, 1994, 1996]. Thus, enhanced clathrin-mediated membrane trafficking may be involved in the entry of other molecules in $PGF_{2\alpha}$ stimulated cells.

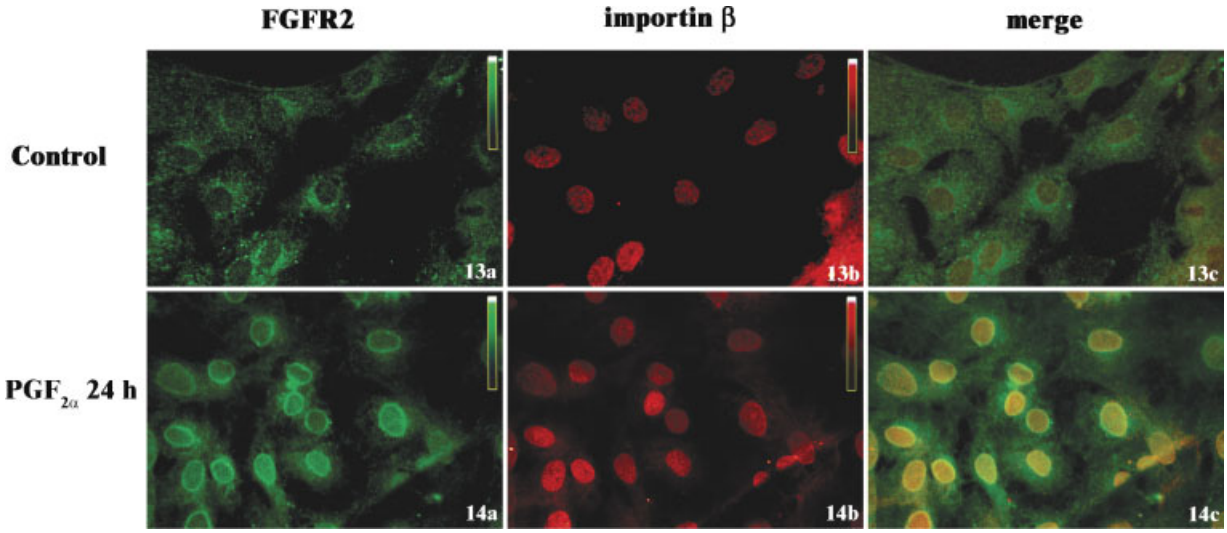

Fig. 13. **a, b, c**: Py1a untreated osteoblasts. Optical section obtained by CLSM. Micrographs showing cells double stained with FGFR2 (green: FITC staining) (a) and importin β (red: Alexa Fluor 594 staining) (b). Merged image (c). The intensity-coded scales, with white being the most intense, are shown on the left. 450×. [Color figure can be viewed in the online issue, which is available at www.interscience.wiley.com.]
Fig. 14. **a,b,c**: Py1a osteoblasts treated for 24 h with $PGF_{2\alpha}$. Optical section obtained by CLSM. Micrographs showing cells double stained with FGFR2 (green: FITC staining) (a) and importin β (red: Alexa Fluor 594 staining) (b). Co-localization of the two signals corresponding to FGFR2 and importin β, assessed by confocal analysis of single optical sections, is shown in yellow pseudo color in the merged image (c). The intensity-coded scales, with white being the most intense, are shown on the left. 450×. [Color figure can be viewed in the online issue, which is available at www.interscience.wiley.com.]

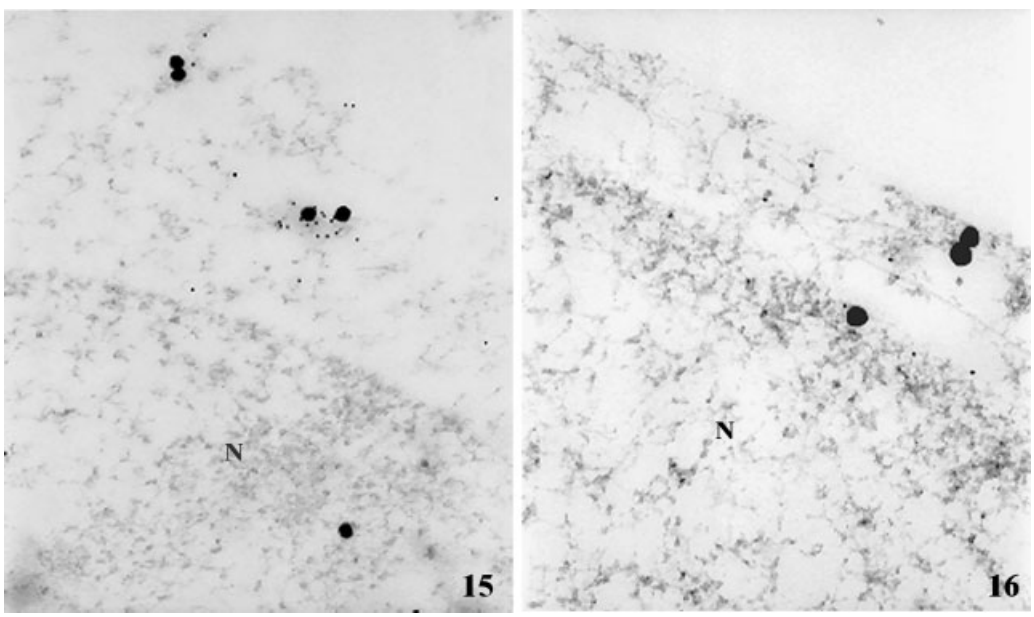

Fig. 15. Double-sided binding of importin β (large gold particles) and FGF-2 (small gold particles) in Py1a osteoblasts pre-treated with PMA for 24 h before administration of $PGF_{2\alpha}$ for other 24 h. Nucleus (N). 36,450×.
Fig. 16. Double-sided binding of importin β (large gold particles) and FGFR2 (small gold particles) (Fig. 16) in Py1a osteoblasts pre-treated with PMA for 24 h before administration of $PGF_{2\alpha}$ for other 24 h. Nucleus (N). 49,300×.

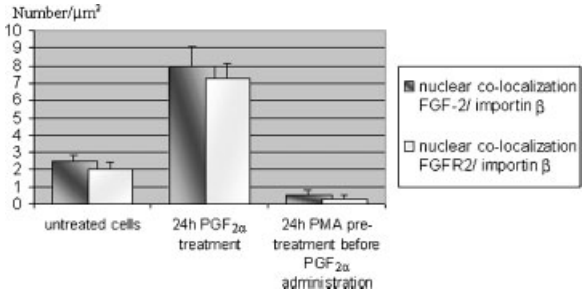

Fig. 17. Statistical analysis of gold particles showing FGF-2/importin β and FGFR2/importin β co-localization in Py1a cell nuclei of untreated cells (2.5 ± 0.5 and 2 ± 0.8, respectively), cells treated with $PGF_{2\alpha}$ for 24 h (8 ± 2 and 7.25 ± 1.5, respectively) and cells treated with PMA pre-treatment before $PGF_{2\alpha}$ administration (0.5 ± 0.5 and 0.25 ± 0.5, respectively). Mean ± SD. $P < 0.05$.

Some studies indicated that FGF-2 could internalize via low affinity sites [Rusnati et al., 1993] and other investigators showed that FGF-2 can be internalized through a direct interaction with cell-surface heparan sulfate suggesting that two distinct pathways of FGF-2 internalization could be involved [Roghani and Moscatelli, 1992]. High and low-affinity binding sites were involved in the internalization of FGF-2 in fibroblasts [Gannoun-Zaki et al., 1991a,b]. Interestingly, recent studies showed that the transmembrane proteoglycan syndecan-4, which functions as low affinity FGF-2 receptor is endocytosed in a non-clathrin mediated manner in endothelial cells upon stimulation with FGF-2 [Tkachenko et al., 2004].

Unstimulated cells did not show co-localized sites for FGF-2 and FGFR2, while cells stimulated with $PGF_{2\alpha}$ exhibited accumulation and co-localization of both proteins. In particular, after 24 h of stimulation, immunogold experiments revealed a characteristic labeling of both FGF-2 and FGFR2 at nuclear pore level. Although growth factor receptors are known to play a role in signal transduction at cell surface level, many of them translocate into the nucleus after ligand-complex formation. In many cases, neither the ligand nor the receptor harbors a nuclear localization signal (NLS) and little is known about the nuclear import of the receptor [Stachowiak et al., 1996; Reilly and Maher,

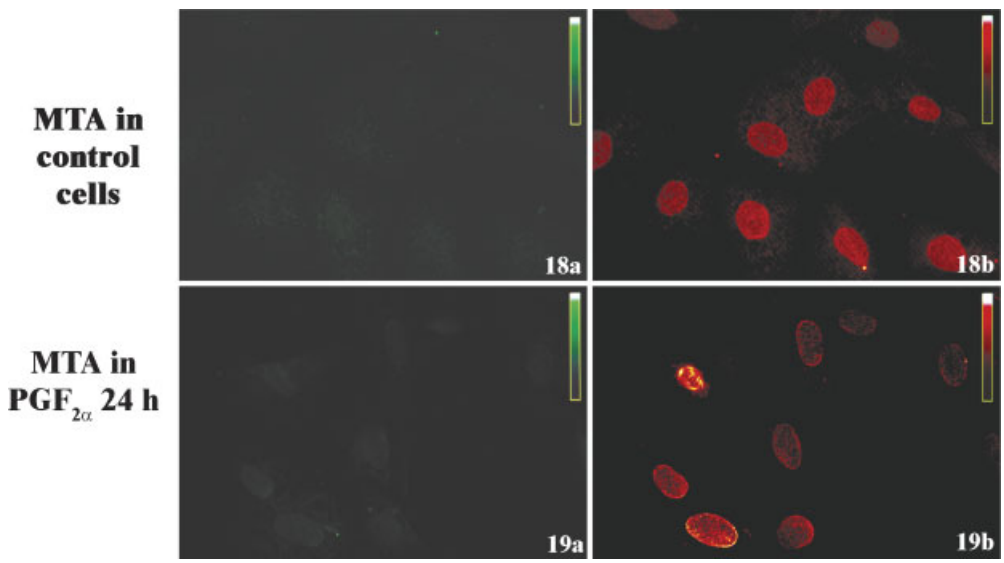

Fig. 18. a, b: MTA pre-treated Py1a osteoblasts. Optical section obtained by CLSM. Micrographs showing cells double stained with FGFR2 (green: FITC staining) (a) and importin β (red: Alexa Fluor 594 staining) (b). The intensity-coded scales, with white being the most intense, are shown on the left. FGFR2 labeling was almost completely abolished by MTA pre-treatment. 450×. [Color figure can be viewed in the online issue, which is available at www.interscience.wiley.com.]

Fig. 19. a, b: MTA pre-treated Py1a osteoblasts before administration of $PGF_{2\alpha}$ for other 24 h. Optical section obtained by CLSM. Micrographs showing cells double stained with FGFR2 (green: FITC staining) (a) and importin β (red: Alexa Fluor 594 staining) (b). The intensity-coded scales, with white being the most intense, are shown on the left. FGFR2 labeling was almost completely abolished by MTA pre-treatment before administration of the effector. 450×. [Color figure can be viewed in the online issue, which is available at www.interscience.wiley.com.]

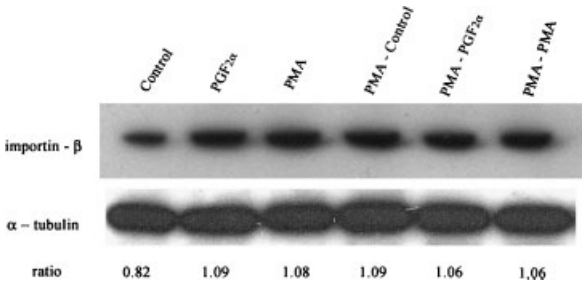

Fig. 20. Western blotting analysis of importin β. Effect of $PGF_{2\alpha}$ and PMA on importin β synthesis. Protein (5 μg) from each sample were subjected to SDS–PAGE, transferred to PVDF membrane and probed with a polyclonal antibody to importin β. Then filters were stripped and riprobed with a monoclonal anti-α-tubulin, mouse ascites fluid to show equal amount of loading.

2001]. Since Py1a osteoblasts stimulated with $PGF_{2\alpha}$ showed co-localized sites for FGF-2 and its receptor 2 and TEM as well as CLSM data showed a close relation between importin β and FGF-2 or FGFR2, we suggest that importin β could be involved in the nuclear import pathway. Furthermore, Western blot analysis demonstrated an increased amount of importin β in Py1a cells stimulated for 24 h with $PGF_{2\alpha}$.

We previously reported that PMA-regulated FGF-2 and FGFR2 expression and localization in Py1a cells by a PKC mediated mechanism [Sabbieti et al., 1999, 2005]. We, therefore, examined the effects of PMA on importin β pathway and we demonstrated that although treatment with PMA increased importin β levels, pre-treatment with this effector did not block importin β increment induced by $PGF_{2\alpha}$ or PMA. These results suggest that other pathways are also involved with PKC to modulate importin β levels.

We previously hypothesized that $PGF_{2\alpha}$ firstly increase FGF-2 mRNA that after translation binds FGFR2 and both proteins are translocated into the nucleus by a PKC-dependent pathway. Indeed, PMA, a specific PKC activator, mimics $PGF_{2\alpha}$-induced perinuclear accumulation and nuclear internalization of FGF-2 and FGFR2 [Sabbieti et al., 2005]. In the present study, a PMA pre-treatment before $PGF_{2\alpha}$ administration, was chosen to confirm a role of importin β in FGFR2/FGF-2 nuclear accumulation. Interestingly, importin β did not show relations with these proteins in the nucleus after PMA pre-treatment. The quantitative study demonstrated that the nuclear gold signals reflecting the FGF-2/importin β and FGFR2/importin β complexes were abrogated in PMA/ $PGF_{2\alpha}$ treated osteoblasts.

Parallel experiments pre-treating cells with MTA, an FGF receptors inhibitor [Chua et al., 2004], showed that, in presence of this inhibitor, FGFR2 is strongly decreased, and also importin β seemed to slightly decrease into the nucleus suggesting a role of this carrier protein in other nuclear events.

The involvement of importin β in nuclear accumulation of proteins in cells was previously reported by other authors who observed that the nuclear import proceeded through nuclear pore complexes and involved a number of distinct pathways; many of which were mediated by importin β-related nuclear transport receptors [Reilly and Maher, 2001]. However, our observation that $PGF_{2\alpha}$ induced nuclear accumulation of importin β is novel and may be of biologic significance. Since several studies have shown that high molecular weight (HMW) nuclear FGF-2 isoforms have NLS and some FGFRs lack a typical NLS [Florkiewicz et al., 1991; Reilly and Maher, 2001], we postulate that upon $PGF_{2\alpha}$ stimulation of Py1a cells, the receptor could be transported into the nucleus in association with HMW FGF-2 by importin β-mediated mechanism. Of relevance to the present study, it was previously reported that in Swiss 3T3 cells, nuclear translocation of fibroblast growth factor receptor-1 (FGFR1) occurs via a mechanism dependent upon importin β [Reilly and Maher, 2001]. Similarly, Stachowiak et al. [1996, 2003] reported that FGFR1 translocated to the nucleus by an importin-β-mediated transport pathway along with its ligand, FGF-2. Although it is reported that FGF-2 signals via both FGFR1 and FGFR2, we never observed labeling of FGFR1 in unstimulated or stimulated Py1a osteoblasts, confirming our previous molecular data [Sabbieti et al., 2005]. Indeed, we have not detected mRNA for other FGFRs in Py1a cells. Moreover, the use of SU5402, a selective inhibitor of FGFR1, further supported the lack of FGFR1 in Py1a cells.

These data are the first to show that importin β appears to be important for FGFR2 nuclear internalization in Py1a osteoblasts.

The nuclear accumulation of FGF-2/FGFR2 could indicate that both proteins may transduce diverse intracellular signals directly to the genome. Peng et al. [2001] reported that the *FGF-2* gene was the first gene regulated by

nuclear FGFR1. Moreover, a nuclear accumulation of another high affinity receptor for FGF-2 (FGFR1) in other in vitro models supports the hypothesis of a direct role for this receptor in DNA replication [Reilly and Maher, 2001; Stachowiak et al., 2003]. Therefore, our findings raise the intriguing possibility that in $PGF_{2\alpha}$ stimulated Py1a osteoblasts, nuclear accumulation of FGF-2/FGFR2 mediated by importin β could plays a role in the direct activation of genes that prepare cells for DNA replication or transcription. Indeed, recently a significant association of transcription sites and hyperphosphorylated RNA pol II with domains of FGFR1 staining was demonstrated [Somanathan et al., 2003]. Further studies are in progress to determine the effects of $PGF_{2\alpha}$/FGF-2/FGFR2 and importin β on osteoblast proliferation.

ACKNOWLEDGMENTS

The authors thank Mrs. S. Cammertoni and Mr. S. Riccioni for excellent technical assistance. We are also grateful to Dr. M. Capacchietti for helping in immunogold procedures. This research was supported by grants from University of Camerino and Fondazione Carima, Italy as well as NIH grant, AG21189 to M.M. Hurley.

REFERENCES

Akimoto N, Sato T, Sakiguchi T, Kitamura K, Kohno Y, Ito A. 2002. Cell proliferation and lipid formation in hamster sebaceous gland cells. Dermatology 204:118–123.

Chua CC, Rahimi N, Forsten-Williams K, Nugent MA. 2004. Heparan sulfate proteoglycans function as receptors for fibroblast growth factor-2 activation of extracellular signal-regulated kinases 1 and 2. Circ Res 94: 316–323.

Conti E, Izaurralde E. 2001. Nucleocytoplasmic transport enters the atomic age. Curr Opin Cell Biol 13:310–319.

Florkiewicz RZ, Baird A, Gonzalez AM. 1991. Multiple forms of bFGF: Differential nuclear and cell surface localization. Growth Factors 4:265–275.

Fujimoto T, Kogo H, Ishiguro K, Tauchi K, Nomura R. 2001. Caveolin-2 is targeted to lipid droplets, a new "membrane domain" in the cell. J Cell Biol 152:1079–1085.

Gannoun-Zaki L, Pieri I, Badet J, Moenner M, Barritault D. 1991a. Internalization of basic fibroblast growth factor by Chinese hamster lung fibroblast cells: Involvement of several pathways. Exp Cell Res 197:272–279.

Gannoun-Zaki L, Pieri I, Badet J, Moenner M, Barritault D. 1991b. Internalization of basic fibroblast growth f actor by CCL39 fibroblast cells. Involvement of heparan sulfate glycosaminoglycans. Ann NY Acad Sci 638:431–433.

Groth C, Lardelli M. 2002. The structure and function of vertebrate fibroblast growth factor receptor 1. Int J Dev Biol 46:393–400.

Görlich D, Kutay U. 1999. Transport between the cell nucleus and the cytoplasm. Annu Rev Cell Dev Biol 15:607–660.

Hurley MM, Marie PJ, Florkiewicz RZ. 2002. Fibroblast growth factor and vascular endothelial fibroblast growth factor families. In: Belizikian J, Raisz LG, Rodan G, editors. Principles of bone biology. San Diego, CA, U.S.A.: Academic Press. p 825–851.

Menghi G, Marchetti L, Bondi AM, Materazzi G. 1997. Contribution of confocal laser scanning microscopy to glycochemistry of mouse and rat submandibular glands by single and double lectin staining. Eur J Histochem 41:91–104.

Nakielny S, Dreyfuss G. 1999. Transport of proteins and RNAs in and out of the nucleus. Cell 99:677–690.

Norrdin RW, Jee WSS, High WB. 1990. The role of prostaglandins in bone in vivo. Prostaglandins Leukot Essent Fatty Acids 41:139–149.

Pearse BM, Robinson MS. 1990. Clathrin, adaptors, and sorting. Annu Rev Cell Biol 6:151–171.

Peng H, Moffett J, Myers J, Fang X, Stachowiak EK, Maher P, Kratz E, Hines J, Fluharty SJ, Mizukoshi E, Bloom DC, Stachowiak MK. 2001. Novel nuclear signaling pathway mediates activation of fibroblast growth factor-2 gene by type 1 and type 2 angiotensin II receptors. Mol Biol Cell 12:449–462.

Pilbeam CC, Harrison JR, Raisz LG. 2002. Fibroblast growth factor and vascular endothelial fibroblast growth factor families. In: Belizikian J, Raisz LG, Rodan G, editors. Principles of bone biology. San Diego CA, U.S.A.: Academic Press. p 979–994.

Prattes S, Horl G, Hammer A, Blaschitz A, Graier WF, Sattler W, Zechner R, Steyrer E. 2000. Intracellular distribution and mobilization of unesterified cholesterol in adipocytes: Triglyceride droplets are surrounded by cholesterol-rich ER-like surface layer structures. J Cell Sci 113:2977–2989.

Raisz LG, Fall PM. 1990. Biphasic effects of prostaglandin E2 on bone formation in cultured fetal rat calvariae: Interaction with cortisol. Endocrinology 126:1654–1659.

Raisz LG, Martin TJ. 1983. Prostaglandins in bone and mineral metabolism. In: Peck WA, editor. Bone and mineral research, Annual 2. Amsterdam: Elsevier. p 286–310.

Raisz LG, Fall PM, Petersen DN, Lichtler A, Kream BE. 1993. Prostaglandin E2 inhibits α_1(I) procollagen gene transcription and promoter activity in the immortalized rat osteoblastic clonal cell line Py1a. Mol Endocrinol 7:17–22.

Reilly JF, Maher PA. 2001. Importin β-mediated nuclear import of fibroblast growth factor receptor: Role in cell proliferation. J Cell Biol 152:1307–1312.

Rodal SK, Skretting G, Garred O, Vilhardt F, van Deurs B, Sandvig K. 1999. Extraction of cholesterol with methyl-beta-cyclodextrin perturbs formation of clathrin-coated endocytic vesicles. Mol Biol Cell 10:961–974.

Roghani M, Moscatelli D. 1992. Basic fibroblast growth factor is internalized through both receptor-mediated and heparan sulfate-mediated mechanisms. J Biol Chem 267:22156–22162.

Rusnati M, Urbinati C, Presta M. 1993. Internalization of basic fibroblast growth factor (bFGF) in cultured endothelial cells: Role of the low affinity heparin-like bFGF receptors. J Cell Physiol 154:152–161.

Sabbieti MG, Marchetti L, Abreu C, Montero A, Hand AR, Raisz LG, Hurley MM. 1999. Prostaglandins regulate the expression of fibroblast growth factor-2 in bone. Endocrinology 140:434–444.

Sabbieti MG, Marchetti L, Hurley MM, Menghi G. 2000. Nuclear and cytoplasmic lectin receptor sites in rat Py1a osteoblasts. Histol Histopathol 15:1107–1117.

Sabbieti MG, Marchetti L, Menghi M, Materazzi S, Menghi G, Raisz LG, Hurley MM. 2001. Prostaglandins regulate FGF-2 and FGF receptor expression and subcellular localization in osteoblasts. Bone 28:S100.

Sabbieti MG, Marchetti L, Gabrielli MG, Menghi M, Materazzi S, Menghi G, Raisz LG, Hurley MM. 2005. Prostaglandins differently regulate FGF-2 and FGF receptor expression and induce nuclear translocation in osteoblasts via MAP kinase. Cell Tissue Res 319:267–278.

Saksela O, Moscatelli D, Sommer A, Rifkin DB. 1988. Endothelial cell-derived heparan sulfate binds basic fibroblast growth factor and protects it from proteolytic degradation. J Cell Biol 107:743–751.

Sandvig K, van Deurs B. 1994. Endocytosis without clathrin. Trends Cell Biol 4:275–277.

Sandvig K, van Deurs B. 1996. Endocytosis, intracellular transport, and cytotoxic action of shiga toxin and ricin. Am Physiol Soc 76:949–965.

Schmid SL. 1997. Clathrin-coated vesicle formation and protein sorting: An integrated process. Annu Rev Biochem 66:511–548.

Somanathan S, Stachowiak EK, Siegel AJ, Stachowiak MK, Berezney R. 2003. Nuclear matrix bound fibroblast growth factor receptor is associated with splicing factor rich and transcriptionally active nuclear speckles. J Cell Biochem 90:856–869.

Stachowiak MK, Maher PA, Joy A, Mordechai E, Stachowiak EK. 1996. Nuclear accumulation of fibroblast growth factor receptors is regulated by multiple signals in adrenal medullary cells. Mol Biol Cell 7:1299–1317.

Stachowiak MK, Fang X, Myers JM, Dunham SM, Berezney R, Maher PA, Stachowiak EK. 2003. Integrative nuclear FGFR1 signaling (INFS) as a part of a universal "feed-forward-and-gate" signaling module that controls cell growth and differentiation. J Cell Biochem 90:662–691.

Tkachenko E, Lutgens E, Stan RV, Simons M. 2004. Fibroblast growth factor 2 endocytosis in endothelial cells proceed via syndecan-4-dependent activation of Rac1 and a Cdc42-dependent macropinocytic pathway. J Cell Sci 117:3189–3199.

van Deurs B, Petersen OW, Olsnes S, Sandvig K. 1989. The ways of endocytosis. Int Rev Cytol 117:130–177.

Yu W, Bozza PT, Tzizik DM, Gray JP, Cassara J, Dvorak AM, Weller PF. 1998. Co-compartmentalization of MAP kinases and cytosolic phospholipase A2 at cytoplasmic arachidonate-rich lipid bodies. Am J Pathol 152:759–769.

Yu W, Cassara J, Weller PF. 2000. Phosphatidylinositide 3-kinase localizes to cytoplasmic lipid bodies in human polymorphonuclear leukocytes and other myeloid-derived cells. Blood 95:1078–1085.